Published in final edited form as:
Cancer Chemother Pharmacol. 2013 April ; 71(4): 999–1011. doi:10.1007/s00280-013-2094-0.

Therapeutic targeting malignant mesothelioma with a novel 6-substituted pyrrolo[2,3-*D*]pyrimidine thienoyl antifolate via its selective uptake by the proton-coupled folate transporter

Christina Cherian, **Sita Kugel Desmoulin**, **Lei Wang**, **Lisa Polin**, **Kathryn White**, **Juiwanna Kushner**, **Mark Stout**, **Zhanjun Hou**, **Aleem Gangjee**[*,€], and **Larry H. Matherly**[*,€]
Graduate Program in Cancer Biology, Wayne State University School of Medicine, Detroit, MI 48201 (SKD, LHM); Department of Oncology, Wayne State University School of Medicine, Detroit, MI 48201 (CC, SKD, LP, KW, JK, ZH, LHM); Molecular Therapeutics Program, Barbara Ann Karmanos Cancer Institute, Detroit, MI 48201 (CC, LP, ZH, LHM); Department of Pharmacology, Wayne State University School of Medicine, Detroit, MI 48201 (LHM); Department of Pediatrics, Children's Hospital of Michigan, Detroit, MI 48201(MS); Division of Medicinal Chemistry, Graduate School of Pharmaceutical Science, Duquesne University, Pittsburgh, PA 15282 (LW, AG)

Abstract

The 5-substituted pyrrolo[2,3-*d*]pyrimidine antifolate pemetrexed (Pmx) is an active agent for malignant pleural mesothelioma (MPM). Pmx is transported into MPM cells by the reduced folate carrier (RFC) and proton-coupled folate transporter (PCFT). We tested the notion that a novel 6-substituted pyrrolo[2,3-*d*]pyrimidine thienoyl antifolate (compound **2**) might be an effective treatment for MPM, reflecting its highly selective membrane transport by PCFT over RFC. Compound **2** selectively inhibited proliferation of a HeLa subline expressing exclusively PCFT (R1-11-PCFT4) over an isogenic subline expressing only RFC (R1-11-RFC6). By outgrowth, H2452 human MPM cells were highly sensitive to the inhibitory effects of compound **2**. By colony-forming assays, following an intermittent (24 h) drug exposure, **2** was cytotoxic. Cytotoxic activity by **2** was due to potent inhibition of glycinamide ribonucleotide formyltransferase (GARFTase) in *de novo* purine biosynthesis, as confirmed by nucleoside protection and *in situ* GARFTase assays with [^{14}C]glycine. Assays with [^{3}H]compound **2** and R1-11-PCFT4 or R1-11-RFC6 cells directly confirmed selective membrane transport by PCFT over RFC. PCFT transport was also confirmed for H2452 cells. In R1-11-PCFT4 and H2452 cells, [^{3}H]compound **2** was metabolized to polyglutamates. Potent *in vivo* efficacy was confirmed toward early- and upstage H2452 xenografts in severe combined immunodeficient mice administered intravenous compound **2**. Our results demonstrate potent antitumor efficacy of compound **2** toward H2452 MPM *in vitro* and *in vivo*, reflecting its efficient membrane transport by PCFT over RFC, synthesis of polyglutamates, and inhibition of GARFTase. Selectivity for non-RFC cellular uptake processes by novel tumor-targeted antifolates such as compound **2** presents an exciting new opportunity for treating solid tumors.

[*]To whom correspondence should be addressed: L.H. Matherly, Molecular Therapeutics Program, Barbara Ann Karmanos Cancer Institute, 110 E. Warren Ave, Detroit, MI 48201. Tel.: 313-578-4280; Fax: 313-578-4287; matherly@karmanos.org. A. Gangjee, Division of Medicinal Chemistry, Graduate School of Pharmaceutical Sciences, Duquesne University, 600 Forbes Avenue, Pittsburgh, PA 15282. 412-396-6070; 412-396-5593 fax; gangjee@duq.edu.
[€] L.H. Matherly and A. Gangjee contributed equally to this work.

DISCLOSURES
None

Keywords

proton-coupled folate transporter; mesothelioma; folate; antifolate; pemetrexed

Introduction

There are an estimated 2500 new cases of malignant pleural mesothelioma (MPM) each year in the United States, approximately 70–80% resulting from workplace exposures to asbestos [4, 16]. In general, symptoms of MPM do not appear until 30–50 years after exposures to asbestos and by the time of diagnosis, the disease is quite advanced. For years, chemotherapy for MPM was ineffective, although several chemotherapy drugs have been shown to generate clinical responses and to prolong patient survivals [8]. Antifolates are active agents for MPM, and pemetrexed (Pmx; Alimta) (Figure 1) is an FDA-approved agent for this disease [12]. While Pmx chemotherapy of MPM (in combination with agents such as cisplatin and gemcitabine) results in improved pulmonary function as well as quality of life, as with other antifolates, clinical efficacy of Pmx can be compromised by toxicity to normal tissues.

In 2006, a previously unknown membrane transporter, the proton-coupled folate transporter (PCFT), was reported to mediate low pH (e.g., pH 5.5) membrane transport of folates into the duodenum [28]. Analogous to folate substrates, antifolates such as methotrexate (Mtx) (Figure 1) and Pmx are generally transport substrates for PCFT, and Pmx is among the best PCFT substrate yet described [17, 38]. However, most classical antifolates including Pmx are also transported by both the reduced folate carrier (RFC; the major folate membrane transporter in tissues and tumors) and folate receptor (FR) α. Recent efforts have begun to focus on discovery of novel cytotoxic antifolates with folate transporter selectivity. Hence, the antifolates PT523 and GW1843U89 are both excellent substrates for RFC but are poorly transported by PCFT [34, 38]. ONX0801 (BGC945) is a small molecule antifolate licensed by Onyx Pharmaceuticals which is a potent inhibitor of thymidylate synthase and a high affinity substrate for FRα but not RFC [10]. More recently, we described cytotoxic 6-substituted pyrrolo[2,3-*d*]pyrimidine thienoyl antifolates (compounds **1** and **2**) (Figure 1) with specificity for cellular uptake by FRs and PCFT over RFC, that inhibit glycinamide ribonucleotide (GAR) formyltransferase (GARFTase), the 1st folate-dependent step in *de novo* purine nucleotide biosynthesis [17, 18, 33, 34]. In *in vivo* efficacy trials with severe combined immunodeficient (SCID) mice harboring subcutaneous (SC) human (KB, IGROV1, HepG2, and HeLa) tumors, both **1** and **2** were potent inhibitors of tumor cell proliferation [17, 18, 33, 34].

The notion of selectively targeting tumors with cytotoxic antifolates via their PCFT membrane transport [15, 18, 20] is especially appealing given the low pH microenvironments of many solid tumors which would seem to favor cellular uptake by PCFT [13, 30, 36]. Indeed, conditions that favor transport of (anti)folate substrates by PCFT are distinct from those for RFC, since PCFT has an acidic pH optimum (pH~5 to 5.5) and shows appreciable transport activity at pH 6.5 to 6.8, whereas RFC exhibits a neutral pH optimum (pH 7.2 to 7.4) with very low levels of transport below pH 7.0 [22, 38]. In terms of tissue specificity, RFC is ubiquitously expressed in normal tissues and tumors [22]. PCFT transcripts are low in most normal human tissues, although PCFT is expressed at high levels in the upper gastrointestinal tract and choroid plexus, as well as in liver and kidney [19, 29, 39]. Notably, a prominent low pH transport route [likely representing human PCFT (hPCFT)], was detected in 29 of 32 human solid tumor cell lines [37]. Moreover, we detected significant levels of hPCFT transcripts in 52 of 53 human solid tumor cell lines (12 from the study by Zhao et al. [37]), seven of which were derived from MPMs [17]. For ten

tumor cell lines, hPCFT protein was detected by western blotting and by [^{3}H]MTX transport at pH 5.5 [18]. hPCFT transcripts were independently confirmed in 8 MPM cell lines by Nutt et al. [23].

The reported clinical efficacy of Pmx toward MPM may in part reflect the expression of PCFT in this tumor. On this basis, we rationalized that novel 6-substituted pyrrolo[2,3-*d*]pyrimidine antifolates with significant PCFT substrate activity and with far greater specificity toward PCFT over RFC than Pmx might offer significant benefits for selective therapeutic targeting tumors including MPM [17, 18, 20, 34, 35]. In this report, we directly test this concept for compound **2**, the lead analog from this series. Our results provide compelling proof-of-principle of antitumor efficacy of compound **2** toward MPM cells both *in vitro* and *in vivo*, reflecting its selective membrane transport by PCFT over RFC and its extensive metabolism to polyglutamates, resulting in potent inhibition of intracellular GARFTase.

Materials and Methods

Materials

[3',5',7-^{3}H]Mtx (20 Ci/mmol), [^{3}H]Pmx (2.5 Ci/mmol), [^{14}C(U)]glycine (107 mCi/mmol), and custom-radiolabeled [^{3}H]compound **2** (1.3 Ci/mmol) were purchased from Moravek Biochemicals (Brea, CA). Leucovorin (LCV) [(6R,S) 5-formyl tetrahydrofolate] was provided by the Drug Development Branch, National Cancer Institute, Bethesda, MD. Pmx [N-{4-[2-(2-amino-3,4-dihydro-4-oxo-7H-pyrrolo[2,3-*d*]pyrimidin-5-yl)ethyl] benzoyl}-*L*-glutamic acid] (Alimta) was provided by Eli Lilly and Co. (Indianapolis, IN). Synthesis and properties of the substituted pyrrolo[2,3-*d*]pyrimidine antifolates, compounds **1** and **2,** were previously described [34, 35]. Other chemicals were obtained from commercial sources in the highest available purities.

Cell lines

HeLa R1-11-RFC6 and R1-11-PCFT4 cells were derived from human RFC (hRFC)- and hPCFT-null R1-11 cells by stable transfection with hemagglutinin (HA)-tagged pZeoSV2(+)-RFC and pZeoSV2(+)-PCFT constructs, respectively [40]. These HeLa sublines along with a R1-11-mock transfectant [transfected with pZeoSV2 (Invitrogen) only; hereafter, designated simply R1-11] and wild-type HeLa cells were gifts from Dr. I. David Goldman (Albert Einstein School of Medicine, Bronx, NY). The H2452 subline is a patient-derived biphasic MPM cell line [24] and was a gift from Dr. Anil Wali (National Cancer Institute). Wild-type and the R1-11 HeLa sublines were cultured as previously described [17, 40]. Routine passage of H2452 cells was in complete RPMI 1640 with 10% fetal bovine serum, antibiotics and 2 mM *L*-glutamine.

For cell proliferation assays, R1-11-PCFT4 and R1-11-RFC6 HeLa cells, and H2452 MPM cells were cultured in folate-free RPMI 1640 (pH 7.2) containing 25 nM LCV, supplemented with 10% dialyzed fetal bovine serum, 2 mM *L*-glutamine and antibiotics for at least 2 weeks. Cells were plated in 96 well culture dishes (5000 cells/well; 200 μl/well) in the above medium with a range of drug concentrations (depending on the compound, dilutions were in DMSO or water with appropriate vehicle controls); cells were incubated for up to 96 h at 37°C in a CO_2 incubator. Metabolically active cells (a measure of cell viability) were assayed with CellTiter-blue™ cell viability assay (Promega; Madison, WI) and a fluorescent plate reader (590 nm emission, 560 nm excitation) for determining IC_{50}s, corresponding to drug concentrations that result in 50% loss of cell growth.

For some of the *in vitro* growth inhibition studies, inhibitory effects of the antifolate drugs on *de novo* thymidylate synthase and purine nucleotide biosynthesis were established by co-incubations with thymidine (10 μM) and adenosine (60 μM), respectively [5-7, 34, 35]. For *de novo* purine biosynthesis, additional protection experiments used 5-amino-4-imidazolecarboxamide (AICA) (320 μM) to distinguish potential inhibitory effects at GARFTase from those at AICA ribonucleotide formyltransferase (AICARFTase) [1, 5, 17, 20].

For colony-forming assays, H2452 cells were treated with a range of concentrations of compound **2** in folate-free RPMI 1640 medium, supplemented with 25 nM LCV, 10% dialyzed fetal bovine serum, penicillin-streptomycin solution, and *L*-glutamine (pH 7.2), in the presence of adenosine (60 μM). After 24 h, the cells were washed (3X) with Hank's balanced salts solution, trypsinized, and 1000 cells were plated in a 60 mm dish in the above media without drug or adenosine. Cells were allowed to outgrow for 10–12 days, at which time the dishes were rinsed with Dulbecco's phosphate-buffered saline (DPBS), 5% trichloroacetic acid (TCA), and borate buffer (10 mM, pH 8.8), followed by 1% methylene blue (in borate buffer). The dishes were again rinsed (3x) with borate buffer, and stained colonies were counted for calculating the percent colony formation relative to the no drug controls.

Real-time RT-PCR analysis of hRFC and hPCFT transcripts

RNAs were isolated from human cell lines including H2452, wild-type HeLa, and R1-11 mock and R1-11-PCFT4 cells using TRIZOL reagent (Invitrogen). cDNAs were synthesized using MuLV reverse transcriptase (Applied Biosystems, Carlsbad, CA) with random hexamers, and purified with the QIAquick PCR Purification Kit (Qiagen, Valencia, CA). Quantitative real-time RT-PCR was performed on a Roche LightCycler 1.2 (Roche, Indianapolis, IN) with gene-specific primers (Table 1S, Supplement) and FastStart DNA Master SYBR Green I enzyme reaction mix (Roche). Transcript levels for hPCFT and hRFC genes were normalized to those for glyceraldehyde-3-phosphate dehydrogenase (GAPDH). External standard curves were constructed for each gene of interest using serial dilutions of linearized templates, prepared by amplification from suitable cDNA templates, subcloning into a TA-cloning vector (PCR-Topo; Invitrogen), and restriction digestions.

In situ GARFT enzyme inhibition assay

Incorporation of [^{14}C(U)]glycine into [^{14}C]formyl GAR as an *in situ* measure of endogenous GARFTase activity in R1-11-PCFT4 and H2452 cells at pH 6.8 was performed using published methods [1, 5], with some modifications exactly as described by Kugel Desmoulin et al. [17].

Transport assays

Transport assays with the R1-11 sublines were routinely performed in suspension using cells grown in spinner flasks, whereas transport assays with H2452 MPM cells used monolayer cultures in 60 mm dishes. For the former, cells were collected by centrifugation, washed with DPBS, and the cell pellets (~1×10^7 cells) were suspended in transport buffer (2 ml) for drug uptake assays in a shaking water bath. pH-dependent uptake of 0.5 μM [^{3}H]Mtx, Pmx, or compound **2** was assayed in cell suspensions over 5 min at 37° C in HEPES-buffered saline (20 mM HEPES, 140 mM NaCl, 5 mM KCl, 2 mM $MgCl_2$, and 5 mM glucose) (HBS) at pH 6.8 or 7.2, or in 4-morphilinopropane sulfonic (MES)-buffered saline (20 mM MES, 140 mM NaCl, 5 mM KCl, 2 mM $MgCl_2$, and 5 mM glucose) (MBS) at pH 5.5 [37]. For some experiments, hRFC transport was measured in "anion-free" buffer (20 mM HEPES, 235 mM sucrose, pH adjusted to ~7.2 with MgO) [14]. Regardless of the transport buffer used, at the end of the incubations, transport was quenched with ice-cold

DPBS. Cells were washed 3 times with ice-cold DPBS, and cellular proteins were solubilized with 0.5 N NaOH. Levels of drug uptake were expressed as pmol/mg cell protein, calculated from direct measurements of radioactivity and protein contents of cell homogenates. Proteins were quantified using Folin-phenol reagent [21].

The pH-dependent uptakes of [^{3}H]Mtx, compound **2**, and [^{3}H]Pmx in H2452 cells were assayed at 37° C in cell monolayers in 60 mm dishes over 5 min at 37°C using HBS and MBS. Processing, quantitation of drug uptake, and analyses of replicate data sets were as described above.

High performance liquid chromatography (HPLC) analysis of polyglutamyl derivatives of compound 2

R1-11-PCFT4 and H2452 cells were grown in complete folate-free RPMI 1640 medium, supplemented with 25 nM LCV and 10% dialyzed fetal bovine serum. Cells were washed with DPBS and incubated in complete RPMI 1640 and 25 mM PIPES/25 mM HEPES (pH 6.8) with 1 μM [^{3}H]compound **2** at 37° C in the presence of 60 μM adenosine. After 16 h, the cells were washed (3X) with ice-cold DPBS, then scraped mechanically into 5 ml of ice-cold DPBS and centrifuged (1800 rpm), and the cell pellets flash frozen. The cell pellets were processed and analyzed for compound **2** polyglutamates exactly as previously described [17, 18], using a Waters 4 μm Nova-Pak C-18 column (3.9 mm × 150 mm) with a Nova-Pak 4 μm C18 guard column, and a Varian 9012 ternary gradient pump and a 9050 Varian UV/Vis detector. Intracellular levels of radiolabeled compounds are expressed as pmol/mg protein, based on calculated percentages of the peaks from the HPLC chromatogram and total pmol/mg of cellular [^{3}H]compound **2** [17, 18].

In vivo efficacy study of compound 2 in H2452 xenografts

Methods for protocol design, drug treatment, toxicity evaluation, data analysis, and quantification of tumor cell kill have been described [3, 25–27] and have been used in our previous studies [34]. Briefly, cultured H2452 cells were implanted subcutaneously (~ 1 × 10^7 cells/flank) to establish a solid tumor xenograft model in female NCR SCID mice (NIH DCT/DTP Animal Production Program, Frederick, MD). Once established, the tumor was maintained in serial passage for a minimum of 5 passage generations before experimentation to allow the development of a consistent tumor growth pattern and stable tumor volume doubling times (Tds) of 2.1 days (folate-replete diet) or 2.3 days (folate-deficient diet). Study mice were maintained on either a folate-deficient diet (Harlan-Teklad; Product ID: TD.00434) or a folate-replete diet (Purina Mills Inc; Lab Diet 5021) starting 15 days before subcutaneous tumor implant for the early stage disease study and 5 days before tumor implant for more advanced stage disease tumors. Folate serum levels were measured prior to the start of therapy and after its completion with a *Lactobacillus casei* bioassay [32] and were found to approximate levels in humans [17, 34, 35]. Individual mouse body weights for each experiment were within 2 g, and all mice weights were over 18 g (advanced stage) or 20 g (early stage) at the start of therapy. The mice were supplied food and water *ad libitum* and were housed in a fully accredited AAALAC animal facility under the care and direction of full-time licensed and board-certified staff veterinarians and veterinary technicians. The animals were pooled and implanted bilaterally subcutaneously with 30–60 mg tumor fragments using a 12-gauge trocar and again pooled before unselective distribution to the various treatment and control groups. The day of tumor implant was day 0. The treatment schedule was every 4 days with 4 injections (q4x4) for all drugs, starting on day 2 for early stage treatment, when the number of cells was small (between 10^7–10^8 cells; below the established limit of palpation). For more advanced stage disease, the tumors were allowed to reach > 250 mg in size before the start of chemotherapy (day 10) with the same injection schedule. All trials had 5 mice per group unless otherwise noted. Standard drugs included

Gemcitabine [(Lilly) dosed at 150 mg/kg] and Cisplatin [(Teva) dosed at 2.8 mg/kg], diluted in 0.9% saline, USP. An organic solvent (ethanol), carrier (Tween-80) and sodium bicarbonate (0.5% v/v) were used to effect solubilization of compound **2** for injection (32 and 24 mg/kg). All drugs were administered by intravenous tail vein injection. The animals were weighed daily and their tumors were measured with a caliper two-to-three times weekly. Mice were sacrificed when the cumulative tumor burden reached 1500 mg (before disease progression impinged on animal heath). Tumor weights were estimated from two dimensional measurements [i.e., tumor mass (in mg) = $(a \times b^2)/2$, where "a" and "b" are the tumor length and width in mm, respectively]. For calculation of end points, both tumors on each mouse were added together, and the total mass per mouse was used. Qualitative and quantitative end points were used to assess antitumor activities including: (i) T/C [expressed as a percent and calculated by dividing the median treated (T) tumor volume by the median control (C) tumor volume multiplied by 100 during the exponential growth phase (approximately 700–1200 mg). A T/C value greater than 42% is considered inactive]; (ii) T-C (tumor growth delay) [where T is the median time in days required for the treatment group tumors to reach a predetermined size (e.g., 1000 mg) and C is the median time in days for the control group tumors to reach the same size; tumor-free survivors are excluded from these calculations]; and (iii) calculation of tumor cell kill [log10 cell kill total (gross) = (T - C)/(3.32)(Td), where (T – C) is the tumor growth delay, as described above, and Td is the tumor volume doubling time in days, estimated from the best fit straight line from a log-linear growth plot of control group tumors in exponential growth (100–800 mg range)].

Statistical analysis

Statistical analyses were performed using GraphPad Prism v. 4.0.

Results

Expression of hPCFT in H2452 human mesothelioma cells

We previously reported that appreciable levels of hPCFT and hRFC transcripts were expressed in seven clinically relevant MPM cell lines by real-time RT-PCR, approximating those in other solid tumor cell lines [17]. FRα levels in the MPM sublines were extremely low and approached the limit of detection, well below the pharmacologically relevant level of FRα in IGROV1 ovarian carcinoma cells. Analogous results were reported by Nutt et al. [23].

We selected the H2452 MPM (biphasic) cell line from our prior study to begin to explore the question of whether the modest level of hPCFT in these cells was sufficient to deliver PCFT-selective cytotoxic antifolates for therapy. For our study we correlated levels of hPCFT transcripts (Figure 2A) and [^{3}H]Mtx transport (0.5 μM, 5 min) at pH 5.5 (Figure 2B) for H2452 MPM cells, compared to those in wild-type HeLa cells and in engineered HeLa cells ectopically expressing hPCFT (R1-11-PCFT4, derived from the hRFC- and hPCFT-null R1-11 HeLa subline) [40]. By this analysis, transport activity at pH 5.5 closely paralleled levels of hPCFT transcripts. While hPCFT protein was detectable in R1-11-PCFT4 on western blots probed with hPCFT antibody, for H2452 cells, endogenous hPCFT protein levels were below the level of reproducible detection (not shown). These results establish the presence of functional hPCFT in H2452 MPM cells.

Selective anti-proliferative activity of the 6-substituted pyrrolo[2,3-*D*]pyrimidine thienoyl antifolate inhibitor compound 2 toward hPCFT-expressing HeLa and H2452 human malignant mesothelioma cells

We previously described the characteristics of PCFT-selective 6-substituted pyrrolo[2,3-*d*]pyrimidine thienoyl antifolates compounds 1 and 2 [17, 18, 34, 35] (Figure 1).

When cells are grown in culture, the tissue culture media pH decreases to ~6.8, sufficient to support appreciable levels of PCFT transport [20, 37]. With engineered CHO cells expressing hPCFT but not hRFC or FRs (R2/PCFT4 cells), compound **2** was an especially potent inhibitor of cell proliferation (IC_{50} ~3 nM), more so than compound **1** (IC_{50} ~43 nM) or Pmx (IC_{50} ~13 nM) [35]. In R1-11 HeLa sublines expressing moderate levels of hPCFT (R1-11-PCFT4) or hRFC (R1-11-RFC6), compound **2**, like compound **1** reported previously [17], was selectively inhibitory toward the hPCFT-expressing cells with limited inhibitory activity toward the hRFC-expressing subline (Figure 3). Compound **2** was ~4-fold more inhibitory than **1** toward R1-11-PCFT4 cells (IC_{50}s of 28.2 nM and 99.2 nM, respectively). Significantly, compound **2** was greater than 35-fold more active toward R1-11-PCFT4 cells than toward the R1-11-RFC6 HeLa subline (IC_{50} of 989 nM), a striking departure from the nearly identical IC_{50}s with Pmx toward these sublines (59.3 nM and 81.7 nM, respectively) [17]. These results establish the potency and growth inhibitory selectivity of compound **2** toward hPCFT- over hRFC-expressing R1-11 cells, analogous to our previous findings with engineered CHO sublines expressing these transporters [35]. Although the sublines derived from R1-11 HeLa cells all express minute amounts of FRα [17], these levels appear to be insufficient to be pharmacologically relevant for cytotoxic drug delivery.

We also tested H2452 MPM cells for sensitivity to growth inhibition by compound **2**. H2452 cells were sensitive to **2**, showing an IC_{50} value (80 nM), similar to that for Pmx (67.3 nM), respectively; Figure 4A and B, respectively). Growth inhibition toward H2452 cells for compound **2** was not impacted by addition of 200 nM folic acid (data not shown), consistent with its FRα-*independent* drug uptake in this MPM cell line model. In colony-forming assays with H2452 cells, pretreatment with **2** for 24 h, followed by plating without drug, showed a time- and concentration-dependent inhibition of colony formation establishing its cytoxicity (Figure 4C). Colony formation was completed abolished at 5 μM compound **2**.

Clearly, for H2452 and R1-11-PCFT cells, both of which express modest levels of hPCFT, compound **2** is a potent inhibitor of cell proliferation. In H2452, this manifests as cytotoxicity.

Compound 2 inhibits cellular GARFTase in H2452 mesothelioma cells

We previously found that compound **2** like compound **1** was a potent inhibitor of *de novo* purine nucleotide biosynthesis in hPCFT-expressing R2/hPCFT4 CHO cells at the step catalyzed by GARFTase, and that inhibition of cell proliferation or colony formation could be ascribed to GARFTase inhibition and depletion of cellular purine nucleotides [35].

To extend these findings to H2452 human MPM cells, we initially tested the impact of nucleoside additions on the growth inhibitions induced by compound **2** and Pmx. Nucleoside protection results for compound **2** are shown in Figure 4B, whereas those for Pmx are in Figure 4A. The inhibitory effects of Pmx were partially reversed by thymidine (10 μM) with a progressive diminution in the extent of protection at higher Pmx concentrations. Neither adenosine (60 μM) nor AICA (320 μM), a precursor of AICA ribonucleotide (AICAR or ZMP) that bypasses the reaction catalyzed by GARFTase [1, 5]), was protective at up to 1000 nM Pmx. Conversely, the growth inhibitory effects of compound **2** toward H2452 cells were completely reversed by adenosine alone, but not at all by thymidine alone. Further, growth inhibition by compound **2** was reversed by AICA. These results establish that compound **2** targets *de novo* purine nucleotide biosynthesis, apparently at the level of GARFTase, in H2452 human mesothelioma cells. Analogous results were obtained for R1-11-PCFT4 HeLa cells treated with compound **2** (Figure 1S, supplement).

We directly measured cellular GARFTase activities in R1-11-PCFT4 HeLa and H2452 MPM cells treated with a range of concentrations of inhibitory antifolates (Pmx, compound

2), using an *in situ* GARFTase activity assay. This sensitive metabolic assay measures incorporation of [^{14}C]glycine into [^{14}C]formyl GAR, the product of GARFTase which accumulates in the presence of azaserine [1, 5, 17, 18, 20]. For both R1-11-PCFT4 and H2452 cells, compound **2** and Pmx inhibited intracellular GARFTase (Figure 5, panels A and B). Compound **2** was more potent than was Pmx toward cellular GARFTase, with IC_{50}s of 25.1 and 44 nM in R1-11-PCFT4 and H2452 cells, respectively, compared with 33.6 and 69.7 nM, respectively, for Pmx. For Pmx, inhibition was incomplete and plateaued at ~80% at the highest drug concentration (500 nM Pmx) for which compound **2** inhibited GARFTase by >95%.

Collectively, these results establish that the inhibition of cell proliferation by compound **2** in hPCFT-expressing human tumor cells, including H2452 MPM cells, reflects its potent inhibition of GARFTase.

Membrane transport of compound 2 in R1-11 and H2452 sublines

Experiments were performed to directly measure hPCFT uptake of [^{3}H]compound **2** (at 0.5 μM) in the H2452 and R1-11 HeLa sublines. Transport was measured at 37°C and pH 5.5 and pH 6.8 over 5 minutes. Transport was also measured for [^{3}H]Pmx.

For R1-11-PCFT4 and H2452 cells, uptake for both [^{3}H]compound **2** and [^{3}H]Pmx was increased (3–4-fold) at pH 5.5 over that at pH 6.8 (Figures 6A, B and D). Transport could be blocked by unlabeled **1** (Figure 6D shows effects of 10 μM compound **1** on [^{3}H]compound **2** uptake in H2452 cells). Uptake of [^{3}H]Pmx and [^{3}H]compound **2** in R1-11-RFC6 cells at pH 5.5 was comparable to that in the transporter-null R1-11 subline. At pH 6.8, reduced albeit still significant uptake of [^{3}H]Pmx in R1-11-PCFT4 and –RFC6 was detected over R1-11 cells, although for [^{3}H]compound **2** net uptake was detected only for R1-11-PCFT4 cells (not R1-11-RFC6 cells). To confirm the contribution of RFC to transport of Pmx (but not **2**), we performed cellular uptake experiments with the R1-11 sublines in “anion-free” (Hepes-sucrose-Mg^{2+}) buffer at pH 7.2 which augments RFC transport due to the lack of competing anions [14]. Results were compared to those for [^{3}H]Mtx and establish that [^{3}H]Mtx and [^{3}H]Pmx but not [^{3}H]compound **2** are transported by RFC (Figure 6C).

The results of direct transport experiments are consistent with those for the *in vitro* cell proliferation assays in Figures 3 and 4, and confirm highly selective membrane transport for compound **2** by hPCFT over hRFC.

Polyglutamylation of compound 2 in HeLa and H2452 MPM sublines

Given the established importance of polyglutamylation to the pharmacologic activity of classical antifolates such as Mtx and Pmx, we measured this metabolism for compound **2** in R1-11-PCFT4 and H2452 cells. For these experiments, cells were incubated with 1 μM [^{3}H]compound **2** for 16 h at pH 6.8 in the presence of 60 μM adenosine. Radiolabeled drug metabolites were extracted and analyzed by HPLC. Up to five radiolabeled metabolites of compound **2** were detected, likely corresponding to di- to hexaglutamyl forms (PG_{2-6}), along with the unmetabolized drug. Total drug accumulations and the distributions of the individual drug forms are summarized in Table 2. These results establish that with both H2452 and R1-11-PCFT4 cells, compound **2** is an excellent substrate for polyglutamylation under conditions (pH 6.8) that favor its membrane transport by hPCFT.

In vivo efficacy studies with H2452 human mesothelioma xenografts and compound 2

We performed *in vivo* studies in SCID mice bearing subcutaneous (SC) xenografts of H2452 tumor to determine the antitumor efficacies of compound **2** under early and late stage (palpable) disease conditions. Mice were maintained on either a standard folate-replete

(control) diet or a folate-deficient diet to decrease serum folates (8–10-fold) to a concentration approximating those in humans [17, 34, 35], then implanted bilaterally with H2452 tumor fragments.

For early stage disease, beginning 2 days after transplant, mice were administered compound **2** (32 mg/kg/dose), gemcitabine (150 mg/kg/dose), or cisplatin (2.8 mg/kg/dose) (drug were given at their optimal highest non-toxic levels) on a Q4dx4 schedule IV. Against H2452 xenografts, compound **2** [0% T/C, 20 day growth delay (T-C), 2.6 logs of cell kill] produced antitumor efficacy clearly superior to gemcitabine (15% T/C, 11 day growth delay, 1.4 logs of cell kill), and cisplatin (52% T/C, 4 day growth delay, 0.5 logs of cell kill). For the efficacious drugs, mice tolerated the treatment regimens well as there were no drug-related lethalities or adverse symptoms other than a reversible weight loss (nadirs sustained for body weight loss ranged from a median 8% for **2** and gemcitabine, to a median 14% for cisplatin). Mice were also administered Pmx (7.2 mg/kg/dose on a Q4dx4 schedule IV for a total dose of 28.8 mg/kg). While this resulted in modest weight loss (median 15.4%), this was *not* accompanied by antitumor activity (97% T/C, no log kill), likely due to elevated serum thymidine in mice [31].

As expected, matched treatment control groups (with H2452 implanted into mice maintained on a folate-replete diet) did not respond appreciably to compound **2** (78% T/C, 3.2% weight gain, 3 day growth delay, and 0.4 log cell kill), whereas efficacy responses for the other drugs were essentially equivalent to those obtained with the folate-deficient diet (17% T/C, 12% weight loss, 13 day growth delay, and 1.9 log cell kill for gemcitabine; 60% T/C, 5.3% weight loss, 7 day growth delay, 1.0 log cell kill for cisplatin). Results for the early stage *in vivo* efficacy experiment are shown in Figure 7A and are summarized in Table 2S in the Supplement.

The efficacy response generated by compound **2** under early stage conditions was sufficient to warrant a second efficacy study with SCID mice bearing more advanced stage (palpable) H2452 tumors (Figure 7B and Table 3S, Supplement). For advanced stage disease, therapy began 10 days post SC transplant of H2452 cells [median tumor burdens were 270–284 mg for mice on the folate-deficient diet and 280–310 mg for mice on the control (folate-replete) diet]. Mice were administered compound **2** (32 mg/kg) or gemcitabine (150 mg/kg) on the same Q4dx4 schedule IV used for the early stage study. Anti-tumor activity for **2** was again substantial (7% T/C, 22 day growth delay, 2.9 log cell kill) and exceeded that for gemcitabine (0% T/C, 17 day growth delay, 2.2 log cell kill). Matched treatment control (folate-replete) groups did not respond to compound **2**. For mice on the folate-deficient diet, both compound **2** and gemcitabine produced a similar number of partial (PR) and complete regressions (CR) (Table 3S, Supplement). Toxicities (weight loss) for both compound **2** and gemcitabine were completely reversible.

Taken together, the results of the *in vivo* efficacy trials with early and advanced H2452 MPM tumors demonstrate potent antitumor activity of compound **2.**

Discussion

MPM is a devastating disease with limited treatment options. The average survival for patients diagnosed with MPM is around 1 year and the 5 year survival approximates 10% [8]. In recent years, newer antifolates such as Pmx and raltitrexed have shown promise, reflected in improved pulmonary function and quality of life, but still result in toxic side effects in patients. High levels of membrane transport into MPM were suggested to explain the chemotherapy activity of Pmx toward this disease [2]. Other drugs have shown activity (as single agents or combined with cisplatin) toward mesothelioma and include gemcitabine,

irinotecan and vinorelbine [8, 9, 16]. Although drugs targeting epiderminal growth factor (Gefitinib), platelet-derived growth factor (Imatinib), vascular endothelial growth factor (thalidomide, bevacizumab), histone deacetylases (SAHA), and the proteasome (bortezomib) have been tested, results have been discouraging [8, 9, 16]. Clearly, there is an urgent need for new and highly selective medications for this disease.

hPCFT is significantly expressed in clinically relevant human MPM cell lines [17, 23]. In this report, we studied the H2452 human malignant mesothelioma subline, a biphasic subtype composed of a mixture of epithelioid and sarcomatoid cells, representing the most aggressive form of this disease [8]. We further document expression of functional hPCFT in H2452 human malignant mesothelioma cells, and explore its potential for tumor targeting with the novel hPCFT-selective antifolate compound **2**. Compound **2** is a prototype and lead analog from an expanded series of 6-substituted pyrrolo[2,3-*d*]pyrimidine thienoyl antifolates [34, 35]. We demonstrated that **2** was an excellent transport substrate for hPCFT in H2452 cells. While **2** is also a substrate for FRα and –β [35], its substrate activity for hRFC in either physiologic or anion-free buffers is nominal. Further, H2452 like other MPM cell lines and primary patient specimens, express minimal amounts of FRα [17, 23].

Following internalization by hPCFT at pH 6.8, compound **2** like other classical antifolates including its 4-carbon analog (compound **1**) and Pmx [17, 18] was extensively metabolized to higher-order polyglutamate conjugates. By analogy with other classical antifolates such as Mtx and Pmx, polyglutamyl drug forms are required for sustained inhibition of tumor cell proliferation [11]. Our present results with H2452 and R1-11-PCFT4 cells strongly imply that the compound **2** polyglutamate forms are potent inhibitors of GARFTase, the 1st folate-dependent enzyme in the *de novo* purine nucleotide biosynthetic pathway. Inhibition of GARFTase *in vitro* by compound **2** results in severe depletion of purine nucleotides (i.e., ATP) [17].

Of particular importance to the broader significance of this work is our finding that hPCFT at the *modest levels* found in the *clinically relevant* H2452 MPM cell line model, and at moderately acidic pH values readily achievable in tumors, can deliver a potent growth inhibitory dose of compound **2** *in vitro*. Cytotoxicity was confirmed in clonogenic assays in which pre-treatment of H2452 cells with compound **2** followed by outgrowth in the absence of drug significantly inhibited colony formation. IC_{50} values for inhibition of H2452 cell proliferation by **2** were similar to those for inhibition of intracellular GARFTase at pH 6.8 by an *in situ* metabolic assay in which [^{14}C]glycine accumulates as [^{14}C]formyl GAR, the GARFTase reaction product.

Finally, our findings were extended *in vivo* with H2452 human tumor xenografts, for which compound **2** was highly active toward both early and more advanced stage disease, as reflected in %T/C, T-C, and gross log kill, exceeding activity produced by first line agents for MPM including gemcitabine and cisplatin.

In summary, we document our continued drug discovery endeavors to identify novel tumor-targeted antifolate drugs that are poorly transported by the ubiquitously-expressed RFC relative to the other major (anti)folate transport systems. Our promising results in a clinically relevant cell line model of human MPM argue that compound **2** is a prototype of an entirely new class of chemotherapy drug that warrants further study of its *in vitro* and *in vivo* drug efficacy in an expanded cohort of human tumors.

Supplementary Material

Refer to Web version on PubMed Central for supplementary material.

Acknowledgments

This study was supported by grants from the National Cancer Institute, National Institutes of health [CA53535, CA125153 and CA152316], a pilot grant from the Barbara Ann Karmanos Cancer Institute, and a grant from the Mesothelioma Applied Research Foundation. Ms. Kugel Desmoulin was supported by a Doctoral Research Award from the Canadian Institutes of Health Research (CIHR).

We thank Dr. Anil Wali (National Cancer Institute, Bethesda, MD) for providing the H2452 mesothelioma cell line. We thank Dr. I. David Goldman (Bronx, NY) for his generous gifts of the R1-11 HeLa cell line series (R1-11-mock, R1-11-RFC6, and R1-11-PCFT4).

Non-standard abbreviations

AICA	5-amino-4-imidazolecarboxamide
AICARFTase	AICA ribonucleotide formyltransferase
CHO	Chinese hamster ovary
DPBS	Dulbecco's phosphate-buffered saline
FR	folate receptor
GAPDH	glyceraldehyde-3-phosphate dehydrogenase
GAR	β-glycinamide ribonucleotide
GARFTase	glycinamide ribonucleotide formyltransferase
HA	hemagglutinin
HBS	HEPES-buffered saline
HEPES	4-(2-hydroxyethyl)-1-piperazine ethanesulfonic acid
hPCFT	human PCFT
HPLC	high performance liquid chromatography
hRFC	human RFC
IC_{50}	fifty percent inhibitory concentration
LCV	leucovorin
MBS	MES-buffered saline
MEM	minimal essential media
MES	4-morphilinopropane sulfonic
MPM	malignant pleural mesothelioma
Mtx	methotrexate
PCFT	proton-coupled folate transporter
PIPES	piperazine-N,N′-bis(2-ethanesulfonic acid)
Pmx	pemetrexed
PVDF	polyvinylidene difluoride
RFC	reduced folate carrier
SC	subcutaneous
SCID	severe combined immunodeficient
SDS-PAGE	sodium dodecyl sulfate polyacrylamide gel electrophoresis

TCA	trichloroacetic acid

References

1. Beardsley GP, Moroson BA, Taylor EC, Moran RG. A new folate antimetabolite, 5,10-dideaza-5,6,7,8-tetrahydrofolate is a potent inhibitor of de novo purine synthesis. J Biol Chem. 1989; 264:328–33. [PubMed: 2909524]
2. Chattopadhyay S, Moran RG, Goldman ID. Pemetrexed: biochemical and cellular pharmacology, mechanisms, and clinical applications. Mol Cancer Ther. 2007; 6:404–17. [PubMed: 17308042]
3. Corbett TH, Valeriote FA, Demchik L, Lowichik N, Polin L, Panchapor C, Pugh S, White K, Kushner J, Rake J, Wentland M, Golakoti T, Hetzel C, Ogino J, Patterson G, Moore R. Discovery of cryptophycin-1 and BCN-183577: examples of strategies and problems in the detection of antitumor activity in mice. Invest New Drugs. 1997; 15:207–18. [PubMed: 9387043]
4. Cugell DW, Kamp DW. Asbestos and the pleura: a review. Chest. 2004; 125:1103–17. [PubMed: 15006974]
5. Deng Y, Wang Y, Cherian C, Hou Z, Buck SA, Matherly LH, Gangjee A. Synthesis and discovery of high affinity folate receptor-specific glycinamide ribonucleotide formyltransferase inhibitors with antitumor activity. J Med Chem. 2008; 51:5052–63. [PubMed: 18680275]
6. Deng Y, Zhou X, Kugel Desmoulin S, Wu J, Cherian C, Hou Z, Matherly LH, Gangjee A. Synthesis and biological activity of a novel series of 6-substituted thieno[2,3-d]pyrimidine antifolate inhibitors of purine biosynthesis with selectivity for high affinity folate receptors over the reduced folate carrier and proton-coupled folate transporter for cellular entry. J Med Chem. 2009; 52:2940–51. [PubMed: 19371039]
7. Fabre G, Fabre I, Matherly LH, Cano JP, Goldman ID. Synthesis and properties of 7-hydroxymethotrexate polyglutamyl derivatives in Ehrlich ascites tumor cells in vitro. J Biol Chem. 1984; 259:5066–72. [PubMed: 6715337]
8. Fennell DA, Gaudino G, O'Byrne KJ, Mutti L, van Meerbeeck J. Advances in the systemic therapy of malignant pleural mesothelioma. Nat Clin Pract Oncol. 2008; 5:136–47. [PubMed: 18227828]
9. Garland LL. Chemotherapy for malignant pleural mesothelioma. Curr Treat Options Oncol. 2011; 12:181–8. [PubMed: 21468683]
10. Gibbs DD, Theti DS, Wood N, Green M, Raynaud F, Valenti M, Forster MD, Mitchell F, Bavetsias V, Henderson E, Jackman AL. BGC 945, a novel tumor-selective thymidylate synthase inhibitor targeted to alpha-folate receptor-overexpressing tumors. Cancer Res. 2005; 65:11721–8. [PubMed: 16357184]
11. Goldman ID, Matherly LH. The cellular pharmacology of methotrexate. Pharmacol Ther. 1985; 28:77–102. [PubMed: 2414788]
12. Hazarika M, White RM, Johnson JR, Pazdur R. FDA drug approval summaries: pemetrexed (Alimta). Oncologist. 2004; 9:482–8. [PubMed: 15477632]
13. Helmlinger G, Yuan F, Dellian M, Jain RK. Interstitial pH and pO2 gradients in solid tumors in vivo: high-resolution measurements reveal a lack of correlation. Nat Med. 1997; 3:177–82. [PubMed: 9018236]
14. Henderson GB, Zevely EM. Use of non-physiological buffer systems in the analysis of methotrexate transport in L1210 cells. Biochem Int. 1983; 6:507–15. [PubMed: 6679721]
15. Hou Z, Kugel Desmoulin S, Etnyre E, Olive M, Hsiung B, Cherian C, Wloszczynski PA, Moin K, Matherly LH. Identification and functional impact of homo-oligomers of the human proton-coupled folate transporter. J Biol Chem. 2011
16. Ismail-Khan R, Robinson LA, Williams CC Jr, Garrett CR, Bepler G, Simon GR. Malignant pleural mesothelioma: a comprehensive review. Cancer Control. 2006; 13:255–63. [PubMed: 17075562]
17. Kugel Desmoulin S, Wang L, Hales E, Polin L, White K, Kushner J, Stout M, Hou Z, Cherian C, Gangjee A, Matherly LH. Therapeutic targeting of a novel 6-substituted pyrrolo [2,3-d]pyrimidine thienoyl antifolate to human solid tumors based on selective uptake by the proton-coupled folate transporter. Mol Pharmacol. 2011; 80:1096–107. [PubMed: 21940787]

18. Kugel Desmoulin S, Wang L, Polin L, White K, Kushner J, Stout M, Hou Z, Cherian C, Gangjee A, Matherly LH. Functional Loss of the Reduced Folate Carrier Enhances the Antitumor Activities of Novel Antifolates with Selective Uptake by the Proton-coupled Folate Transporter. Mol Pharmacol. 2012 in press.
19. Kugel Desmoulin S, Wang Y, Tait L, Hou Z, Cherian C, Gangjee A, Matherly LH. Expression profiling of the major folate facilitative transporters in human tumors and normal tissues. Abstracts, American Association for Cancer Research. 2010; 51:1103.
20. Kugel Desmoulin S, Wang Y, Wu J, Stout M, Hou Z, Fulterer A, Chang MH, Romero MF, Cherian C, Gangjee A, Matherly LH. Targeting the proton-coupled folate transporter for selective delivery of 6-substituted pyrrolo[2,3-d]pyrimidine antifolate inhibitors of de novo purine biosynthesis in the chemotherapy of solid tumors. Mol Pharmacol. 2010; 78:577–87. [PubMed: 20601456]
21. Lowry OH, Rosebrough NJ, Farr AL, Randall RJ. Protein measurement with the Folin phenol reagent. J Biol Chem. 1951; 193:265–75. [PubMed: 14907713]
22. Matherly LH, Hou Z, Deng Y. Human reduced folate carrier: translation of basic biology to cancer etiology and therapy. Cancer Metastasis Rev. 2007; 26:111–28. [PubMed: 17334909]
23. Nutt JE, Razak AR, O'Toole K, Black F, Quinn AE, Calvert AH, Plummer ER, Lunec J. The role of folate receptor alpha (FRalpha) in the response of malignant pleural mesothelioma to pemetrexed-containing chemotherapy. Br J Cancer. 2010; 102:553–60. [PubMed: 20051956]
24. Pass HI, Stevens EJ, Oie H, Tsokos MG, Abati AD, Fetsch PA, Mew DJ, Pogrebniak HW, Matthews WJ. Characteristics of nine newly derived mesothelioma cell lines. Ann Thorac Surg. 1995; 59:835–44. [PubMed: 7695406]
25. Polin, L.; Corbett, TH.; Roberts, BJ.; Lawson, AJ.; Leopold, WR., III; White, K.; Kusner, J.; Paluch, J.; Hazeldine, S.; Moore, R.; Rake, J.; Horwitz, JP. Tumor Models in Cancer Research. Humana Press, Inc; Totowa, NJ: 2011. Transplantable Syngeneic Tumors: Solid Tumors of Mice; p. 43-78.
26. Polin L, Valeriote F, White K, Panchapor C, Pugh S, Knight J, LoRusso P, Hussain M, Liversidge E, Peltier N, Golakoti T, Patterson G, Moore R, Corbett TH. Treatment of human prostate tumors PC-3 and TSU-PR1 with standard and investigational agents in SCID mice. Invest New Drugs. 1997; 15:99–108. [PubMed: 9220288]
27. Polin L, White K, Kushner J, Paluch J, Simpson C, Pugh S, Edelstein MK, Hazeldine S, Fontana J, LoRusso P, Horwitz JP, Corbett TH. Preclinical efficacy evaluations of XK-469: dose schedule, route and cross-resistance behavior in tumor bearing mice. Invest New Drugs. 2002; 20:13–22. [PubMed: 12003190]
28. Qiu A, Jansen M, Sakaris A, Min SH, Chattopadhyay S, Tsai E, Sandoval C, Zhao R, Akabas MH, Goldman ID. Identification of an intestinal folate transporter and the molecular basis for hereditary folate malabsorption. Cell. 2006; 127:917–28. [PubMed: 17129779]
29. Qiu A, Min SH, Jansen M, Malhotra U, Tsai E, Cabelof DC, Matherly LH, Zhao R, Akabas MH, Goldman ID. Rodent intestinal folate transporters (SLC46A1): secondary structure, functional properties, and response to dietary folate restriction. Am J Physiol Cell Physiol. 2007; 293:C1669–78. [PubMed: 17898134]
30. Raghunand N, Altbach MI, van Sluis R, Baggett B, Taylor CW, Bhujwalla ZM, Gillies RJ. Plasmalemmal pH-gradients in drug-sensitive and drug-resistant MCF-7 human breast carcinoma xenografts measured by 31P magnetic resonance spectroscopy. Biochem Pharmacol. 1999; 57:309–12. [PubMed: 9890558]
31. van der Wilt CL, Backus HH, Smid K, Comijn L, Veerman G, Wouters D, Voorn DA, Priest DG, Bunni MA, Mitchell F, Jackman AL, Jansen G, Peters GJ. Modulation of both endogenous folates and thymidine enhance the therapeutic efficacy of thymidylate synthase inhibitors. Cancer Res. 2001; 61:3675–81. [PubMed: 11325838]
32. Varela-Moreiras G, Selhub J. Long-term folate deficiency alters folate content and distribution differentially in rat tissues. J Nutr. 1992; 122:986–91. [PubMed: 1552373]
33. Wang L, Cherian C, Kugel Desmoulin S, Mitchell-Ryan S, Hou Z, Matherly LH, Gangjee A. Synthesis and biological activity of 6-substituted pyrrolo[2,3-d]pyrimidine thienoyl regioisomers as inhibitors of de novo purine biosynthesis with selectivity for cellular uptake by high affinity

folate receptors and the proton-coupled folate transporter over the reduced folate carrier. J Med Chem. 2012

34. Wang L, Cherian C, Kugel Desmoulin S, Polin L, Deng Y, Wu J, Hou Z, White K, Kushner J, Matherly LH, Gangjee A. Synthesis and antitumor activity of a novel series of 6-substituted pyrrolo[2,3-d]pyrimidine thienoyl antifolate inhibitors of purine biosynthesis with selectivity for high affinity folate receptors and the proton-coupled folate transporter over the reduced folate carrier for cellular entry. J Med Chem. 2010; 53:1306–18. [PubMed: 20085328]
35. Wang L, Kugel Desmoulin S, Cherian C, Polin L, White K, Kushner J, Fulterer A, Chang MH, Mitchell-Ryan S, Stout M, Romero MF, Hou Z, Matherly LH, Gangjee A. Synthesis, biological, and antitumor activity of a highly potent 6-substituted pyrrolo[2,3-d]pyrimidine thienoyl antifolate inhibitor with proton-coupled folate transporter and folate receptor selectivity over the reduced folate carrier that inhibits beta-glycinamide ribonucleotide formyltransferase. J Med Chem. 2011; 54:7150–64. [PubMed: 21879757]
36. Wike-Hooley JL, Haveman J, Reinhold HS. The relevance of tumour pH to the treatment of malignant disease. Radiother Oncol. 1984; 2:343–66. [PubMed: 6097949]
37. Zhao R, Gao F, Hanscom M, Goldman ID. A prominent low-pH methotrexate transport activity in human solid tumors: contribution to the preservation of methotrexate pharmacologic activity in HeLa cells lacking the reduced folate carrier. Clin Cancer Res. 2004; 10:718–27. [PubMed: 14760095]
38. Zhao R, Goldman ID. The molecular identity and characterization of a Proton-coupled Folate Transporter--PCFT; biological ramifications and impact on the activity of pemetrexed. Cancer Metastasis Rev. 2007; 26:129–39. [PubMed: 17340171]
39. Zhao R, Matherly LH, Goldman ID. Membrane transporters and folate homeostasis: intestinal absorption and transport into systemic compartments and tissues. Expert Rev Mol Med. 2009; 11:e4. [PubMed: 19173758]
40. Zhao R, Qiu A, Tsai E, Jansen M, Akabas MH, Goldman ID. The proton-coupled folate transporter: impact on pemetrexed transport and on antifolates activities compared with the reduced folate carrier. Mol Pharmacol. 2008; 74:854–62. [PubMed: 18524888]

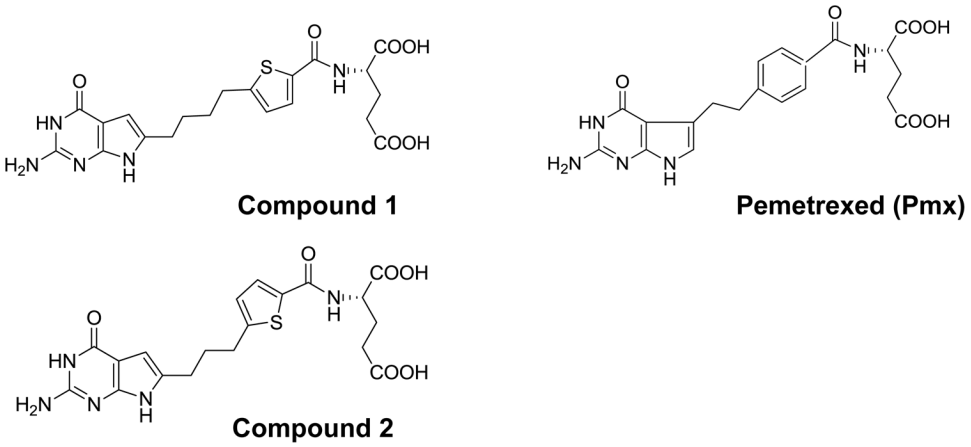

Figure 1.
Structures of 6-substituted pyrrolo[2,3-*D*]pyrimidine thienoyl antifolates compound 1 and compound 2, along with Pmx.

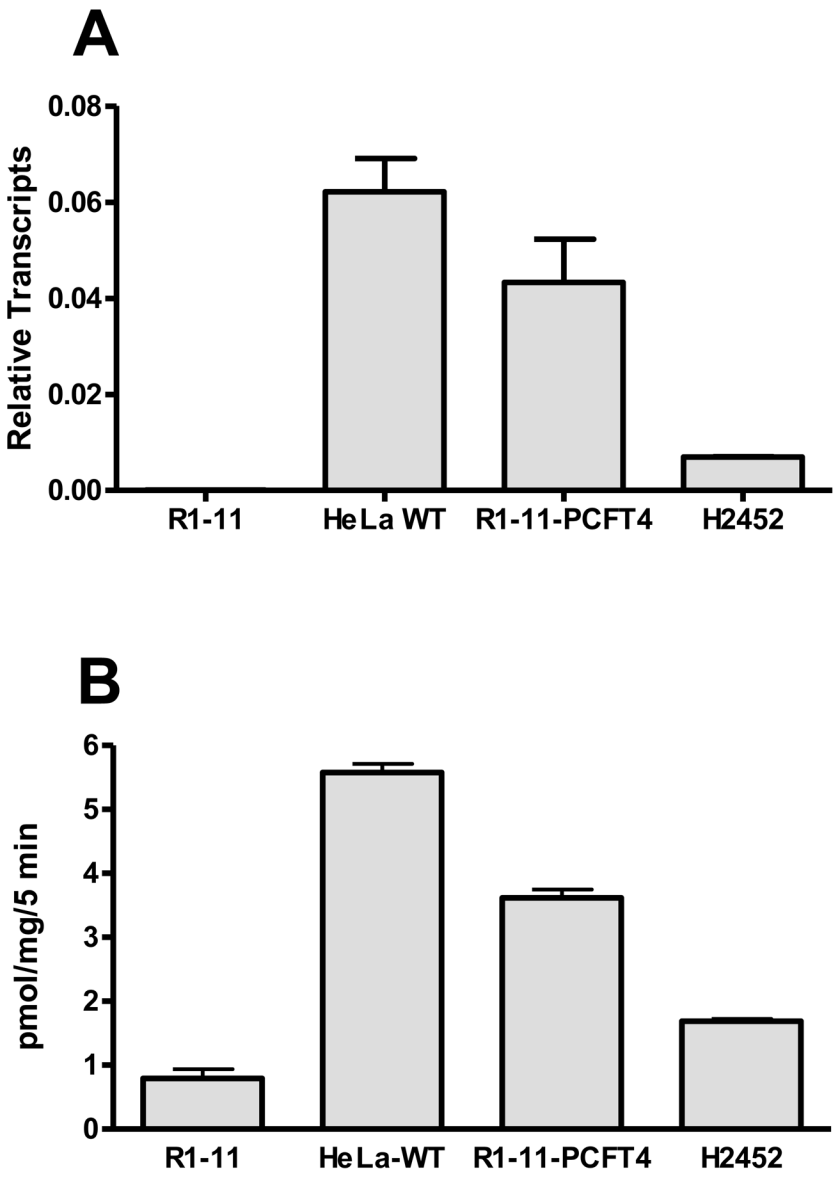

Figure 2. hPCFT expression in human solid tumor cell lines

Panel A: Results are shown for real-time RT-PCR analysis of hPCFT transcripts in R1-11, HeLa wild-type (WT), R1-11-PCFT4 and H2452 cells, normalized to levels of GAPDH transcripts. *Panel B*: Transport was measured in R1-11, HeLa wild-type, R1-11-PCFT4, and H2452 cells over 5 minutes at 37°C with [^{3}H]Mtx at 0.5 μM in pH 5.5 buffer. Internalized [^{3}H]Mtx was normalized to total cell proteins and results are expressed as pmol/mg cell protein. Results are presented as mean values plus/minus ranges from 2–3 experiments.

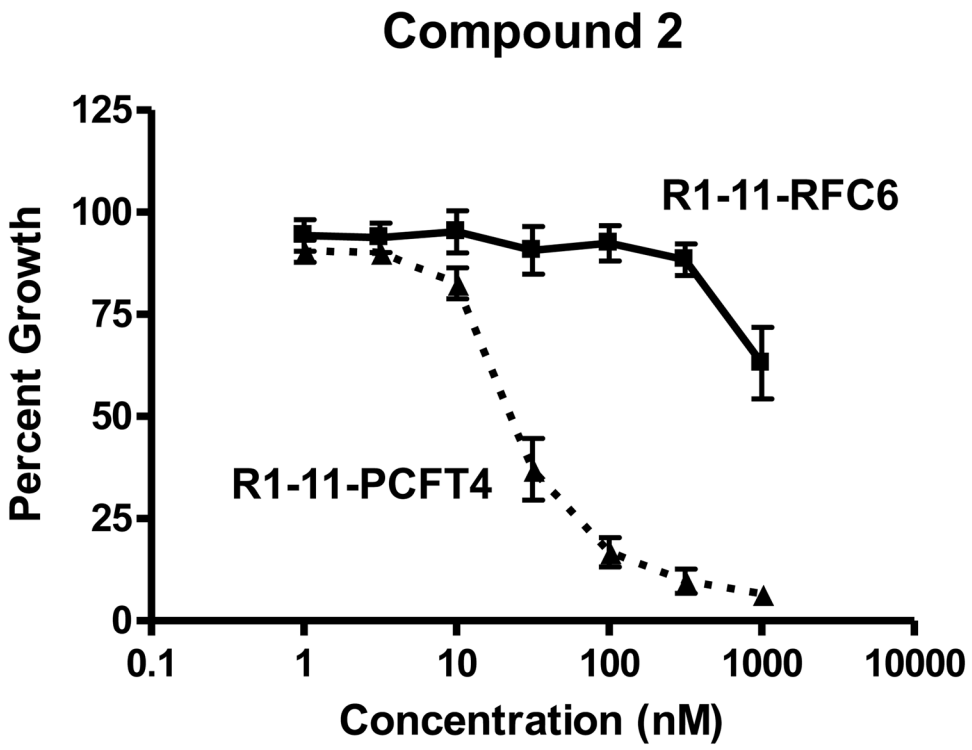

Figure 3. Characterization of growth inhibition by compound 2

Growth inhibition curves for R1-11-PCFT4 and -RFC6 cells treated continuously with compound **2** are shown. Cells were plated (5000 cells/well) in folate-free RPMI 1640 medium with 10% dialyzed serum, antibiotics, *L*-glutamine, and 25 nM LCV. Relative cell numbers were quantitated after 96 h as described in Materials and Methods. IC_{50} values (as mean values ± SEM) were 28.2 (± 7) nM for R1-11-PCFT4 and 989(± 11) nM for R1-11-RFC6 cells (n=3).

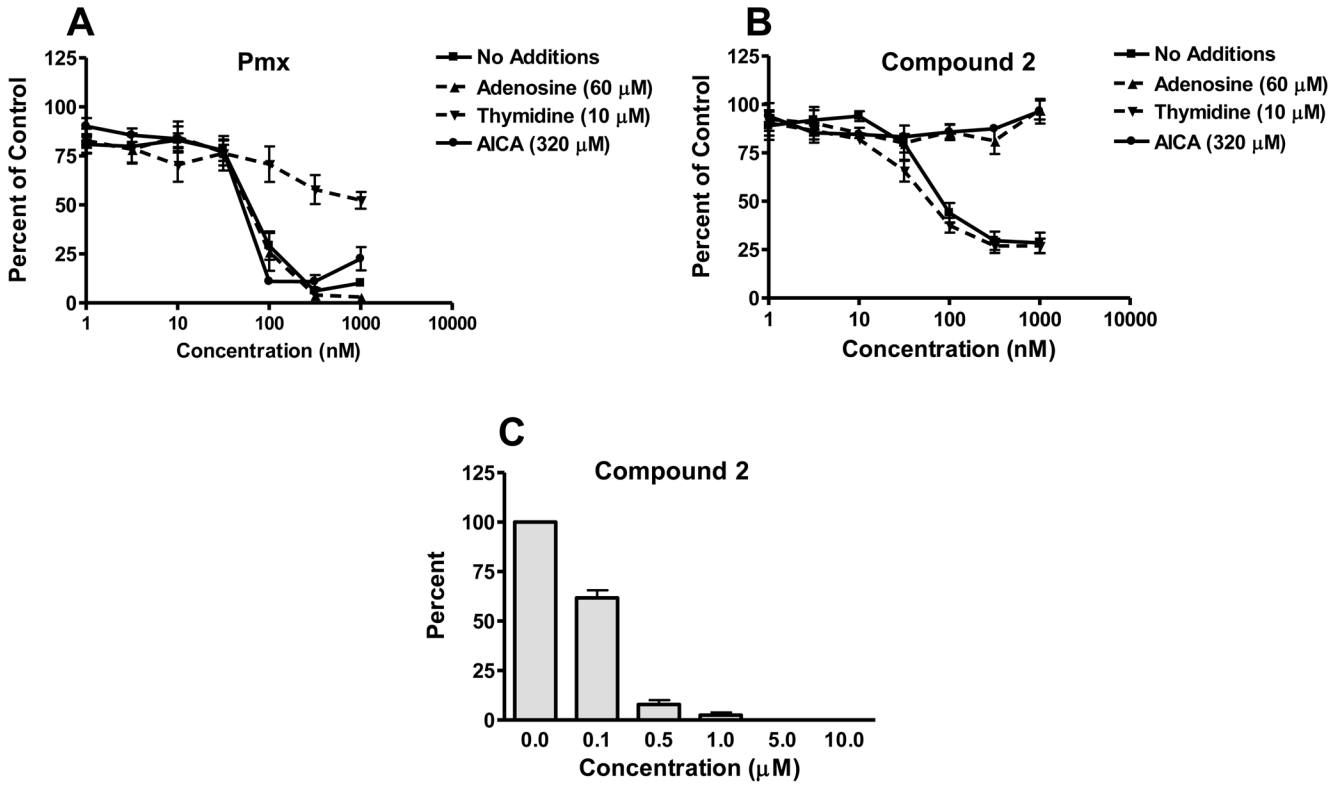

Figure 4. Protection of H2452 cells from growth inhibition by Pmx and the 6-substituted pyrrolo[2,3-*D*] pyrimidine thienoyl antifolate 2 in the presence of nucleosides and AICA and H2452 colony forming assays

Panels A and B: Inhibition of cell proliferation was measured for H2452 human MPM cells over a range of concentrations of Pmx (*panel A*) or compound 2 (*panel B*), in the presence of adenosine (60 μM), thymidine (10 μM), or AICA (320 μM), as described in Materials and Methods. Results were normalized to cell density in the absence of drug. IC_{50} values for growth inhibition in the absence of nucleoside additions were 80.0 ± 15.2 nM for compound **2** and 67.3 ± 9.9 nM for Pmx (n=3). In *panel C*, results (presented as mean values ± SEM) for triplicate colony forming assays in which cells were pretreated 24 h with a range of concentrations of compound **2** (in the presence of 60 μM adenosine), washed with DPBS, and plated (1000 cells) in the absence of antifolate or adenosine for 10–12 days. Colonies were stained with methylene blue and counted for calculation of percent colony formation relative to control cells treated with adenosine but no antifolate. The IC_{50} value for inhibition of colony formation following discontinuous treatment with compound **2** was 0.13 ± 0.012 μM.

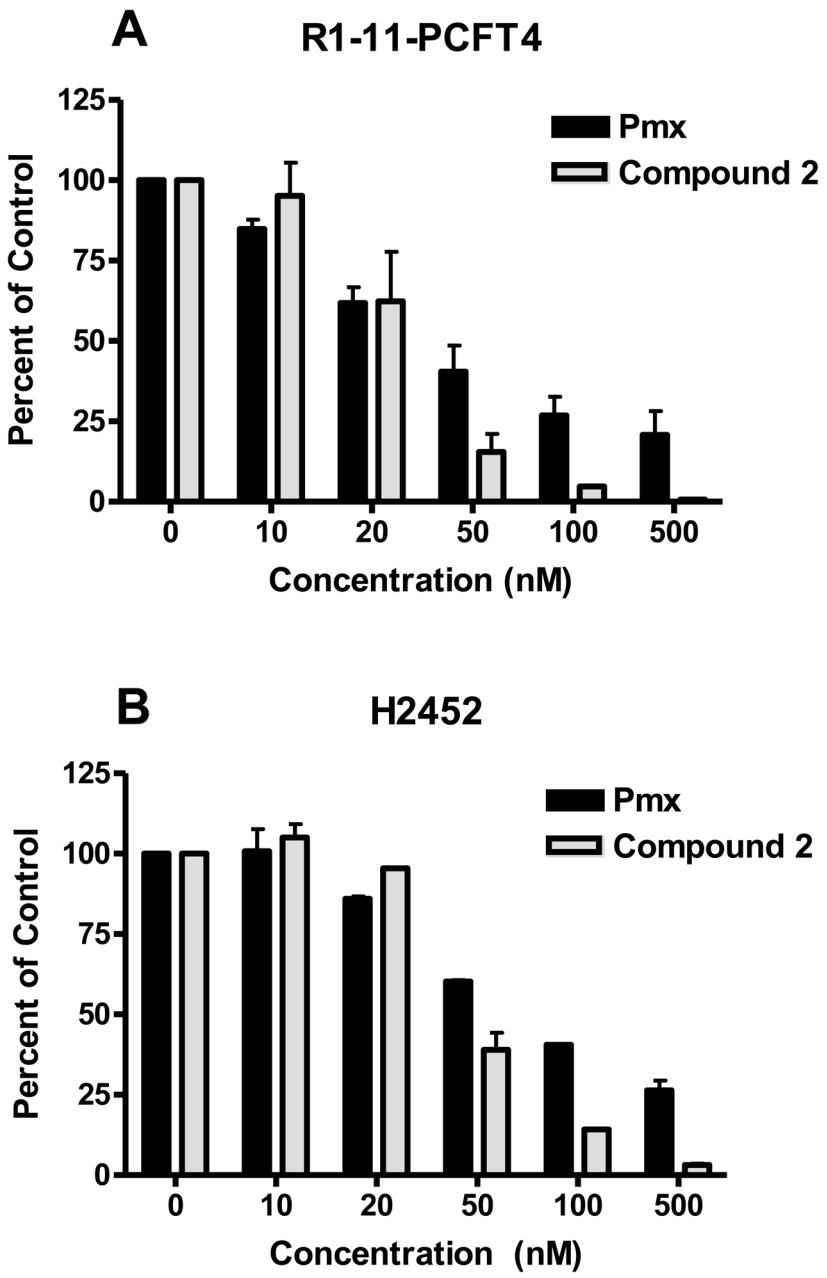

Figure 5. In situ

GARFTase inhibition by compound 2 and Pmx in R1-11-PCFT4 and H2452 cells. GARFTase activity and inhibition were evaluated *in situ* with R1-11-PCFT4 cells (*panel A*) and H2452 cells (*panel B*). For both cell lines, cells were treated with drug for 16 h at pH 6.8 in complete folate-free RPMI 1640 supplemented with 10% dialyzed fetal bovine serum and 25 mM HEPES/25 mM PIPES before incubating in the presence of 4 μM azaserine for 30 min, followed by [^{14}C]glycine and *L*-glutamine treatment. After 8 h, radioactive metabolites were extracted and analyzed. Methods including those for quantifying [^{14}C]formyl GAR are described under Materials and Methods. Results are presented for duplicate experiments (as average values plus/minus ranges) as percentages of vehicle controls over a series of drug concentrations. For H2452 cells, IC_{50}s for GARFTase

inhibition were 44 nM ± 6 nM and 68.3 ± 0.8 nM for compound **2** and Pmx, respectively; for R1-11-PCFT4 cells, these values were 25.1 ± 11.8 nM and 33.6 ± 15.2 nM, respectively.

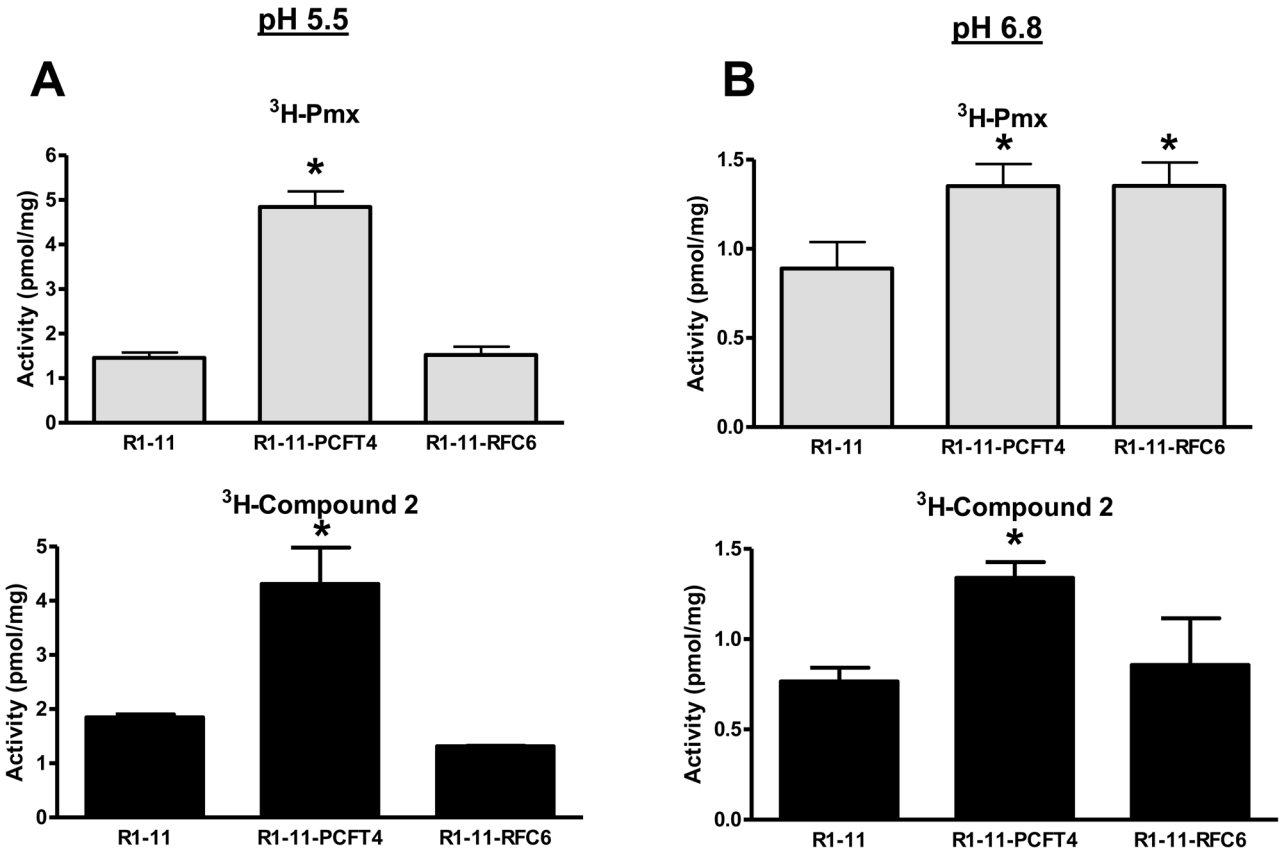

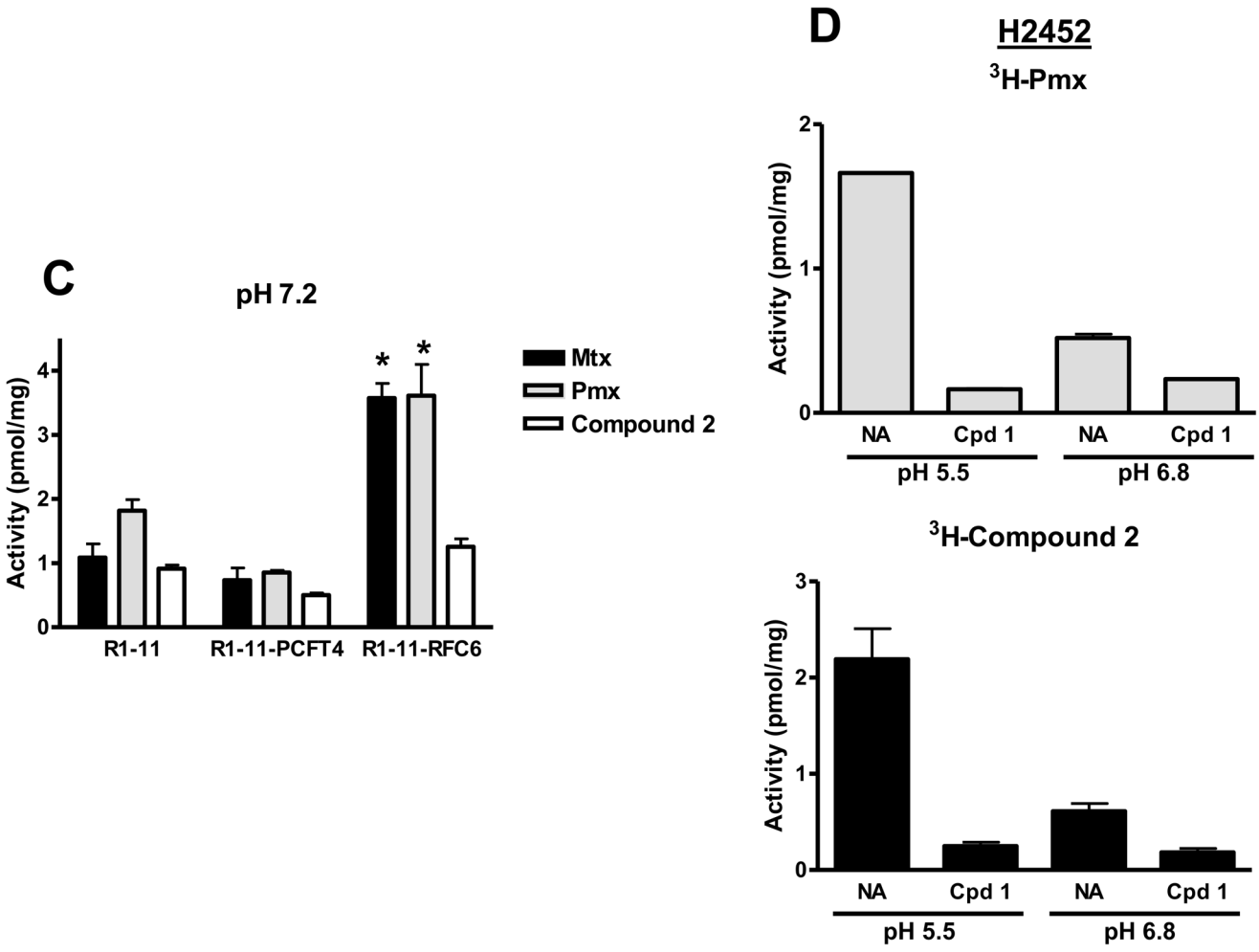

Figure 6. pH-dependent transport of Pmx and compound 2 in R1-11 HeLa and H2452 MPM sublines

Panels A and B: Cellular uptake was measured over 5 minutes in R1-11 mock (labeled R1-11), R1-11-PCFT4, and R1-11-RFC6 HeLa cells at 37°C with [^{3}H]Pmx and [^{3}H]compound **2** (both at 0.5 μM) in pH 5.5 (*panel A*) and pH 6.8 (*panel B*) buffers. Details are provided in Materials and Methods. In *panel C*, cellular uptakes of [^{3}H]Mtx, [^{3}H]Pmx, and [^{3}H]compound **2** (each at 0.5 μM) were measured over 5 minutes at pH 7.2 in anion-free Hepes-sucrose-Mg^{2+} buffer. For panels A–C, statistically significant differences ($p < 0.05$) in [^{3}H]Pmx or compound **2** uptake levels between R1-11-PCFT or R1-11-RFC6 and those in R1-11 cells are noted (*). In *panel D*, cellular uptake was measured over 5 min in H2452 MPM cells for [^{3}H]Pmx and [^{3}H]compound **2** (both at 0.5 μM) at pH 5.5 and pH 6.8 in the absence and presence of 10 μM unlabeled compound **1**. For both [^{3}H]Pmx and [^{3}H]compound **2**, differences in the absence

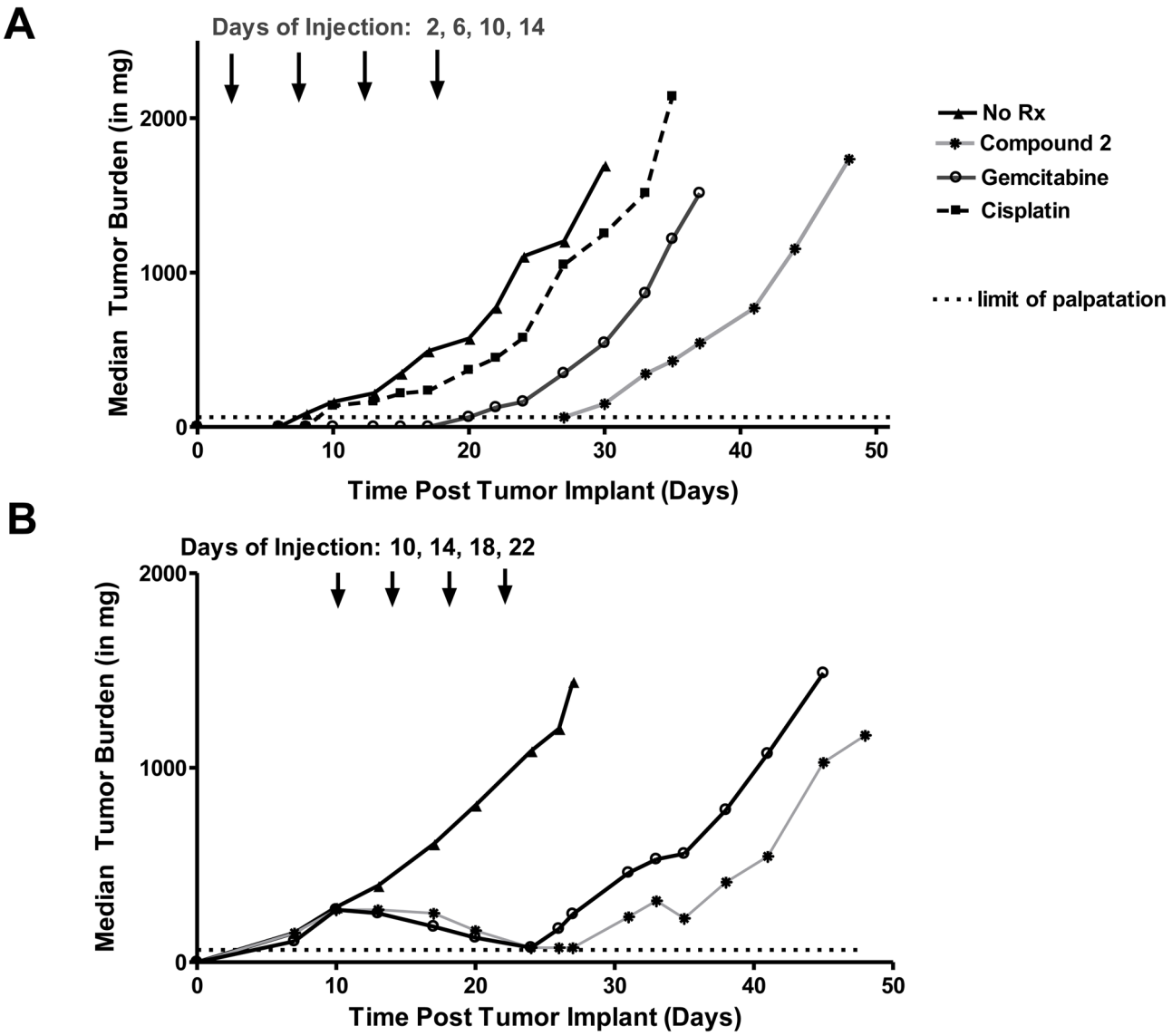

Figure 7.

Table 1

HPLC analysis of polyglutamyl derivatives of [^{3}H]Compound 2 in H2452 and R1-11-PCFT4 cells at pH 6.8

H2452 and R1-11-PCFT cells were treated with 1 μM of [^{3}H]compound **2** at pH 6.8 in the presence of adenosine (60 μM) for 16 h. Polyglutamates (PG) of compound **2** were extracted and analyzed by reverse-phase HPLC, as described in Materials and Methods. Percent monoglutamate and polyglutamate drug forms (labeled as PG_n) are expressed in units of pmol/mg cell protein and the percentages of the total intracellular drug forms are noted with parentheses. These results are for a representative experiment performed in duplicate.

	Compound 2	
	H2452 (pmol/mg)	**R1-11-PCFT4 (pmol/mg)**
Total	6.30	7.77
PG_6	0.54 (8.52%)	1.16 (14.94%)
PG_5	1.29 (20.42%)	3.12 (40.14%)
PG_4	1.43 (22.75%)	0.23 (2.95%)
PG_3	0.26 (4.04%)	0.32 (4.09%)
PG_2	0.39 (6.11%)	0.66 (8.45%)
PG_1	2.7 (39.09%)	2.48 (31.86%)